PyCBC Live $p_{\rm astro}$ for O4

LIGO Document T2300168-v2

Thomas Dent, for the LVK PyCBC team

May 31, 2023

1 Context and basic setup

The probability of astrophysical origin $p_{\rm astro}$, for background (noise) and foreground (signal) processes described by rate densities of events $R_N(\vec{\kappa})$, $R_S(\vec{\kappa})$, is given by [1]

$$\frac{p_{\rm astro}}{1-p_{\rm astro}} \equiv \frac{p_{\rm astro}}{p_{\rm terr}} = \frac{R_S(\vec{\kappa})}{R_N(\vec{\kappa})}, \tag{1}$$

$$p_{\rm astro} = \frac{R_S(\vec{\kappa})}{R_S(\vec{\kappa}) + R_N(\vec{\kappa})}. \tag{2}$$

These densities will vary over the parameter space of triggers $\vec{\kappa}$ produced by a search pipeline. We would like to extract the main dependencies and implement them in some approximation using information available within the compact binary merger search PyCBC Live [2, 3]. Note that the densities should be expressed over the same space of coordinates, or if in different coordinates we need a Jacobian to transform between them.

The basic dependencies to be considered are:

- The densities of signal and noise vary over the bank parameters (binary masses, spins) – we denote these parameters schematically as θ.
- The densities vary over the trigger ranking statistic ρ_c which is a 'SNR-like' variable, i.e. proportional to quadrature sum of SNRs over detectors, up to corrections due to chisq and network consistency.

We can factorize the densities into a total density of noise or signal triggers (above some threshold in SNR or ρ_c) over the bank $r_N(\theta)$, $r_S(\theta)$, times the relative density of noise/signal at a given position in the bank

$$R_{S,N} = r_{S,N}(\theta) f_{S,N}(\rho_c|\theta), \tag{3}$$

where $f_{S,N}(\rho_c|\theta)$ are normalised PDFs (for triggers above the chosen threshold).

2 Modelling event PDFs over ranking statistic

For the background PDF, the ranking statistic model used for O2-O3 offline analysis [4, 5] considers exponential falloffs in the *single-detector* SNR-like statistics

$$p(\hat{\rho}_D|\theta) \sim \exp(-\alpha_D(\theta)\hat{\rho}_D) \tag{4}$$

where α_D is a detector- and template-dependent fit coefficient. However, the online analysis ranking [4] does not consider any such variation of background distributions. Instead, it scales simply as the quadrature sum of SNR-like statistics over detectors.

The simplest resulting approximate model of the background distribution of $\rho_c \simeq (\hat{\rho}_A^2 + \hat{\rho}_B^2)^{1/2}$ for detectors A and B is

$$f_N(\rho_c|\theta) = p(\rho_c|\theta) \simeq \alpha_c \exp(-\alpha_c(\rho_c - \rho_{\rm th})) \quad (\rho_c > \rho_{\rm th}) \tag{5}$$

where α_c remains to be determined (e.g. it might be fit to distributions obtained from online background estimation; see also [6]). For the case $\hat{\rho}_A \simeq \hat{\rho}_B$, we find $\alpha_c \simeq (\alpha_A + \alpha_B)/\sqrt{2}$.

For lower-mass templates corresponding to systems of interest for followup observations, we find $\alpha_c = 6$ to be a reasonable approximation. Generally, α_A decreases for higher masses, so setting $\alpha_c = 6$ results in a conservative (high) estimate of f_N for high-mass templates. It is to be investigated whether allowing α_c to be dependent on template parameters or on detector combination produces a more accurate model.

We approximate the signal PDF by the ideal signal SNR distribution $p(\rho) \sim \rho^{-4}$. Applying this to the ranking statistic neglects threshold effects and other contributions to the statistic beyond SNR, but is unlikely to be out by a large factor. Thus, we take

$$f_S(\rho_c) \simeq 3\rho_{\rm th}^3 \rho_c^{-4} \quad (\rho_c > \rho_{\rm th}), \tag{6}$$

independent of the template parameters.

3 Modelling template-dependent rate densities

In O3 the bank parameter space was split into 3 bins by template chirp mass [7]. This is easily implemented, but (at least for a small number of bins) possibly not a good approximation of the actual signal distribution. We can consider improving the bin configuration.

Due to the highly non-uniform distribution of both signals and templates/noise events over the mass space, we consider an explicit model of these distributions $r_{S,N}(\theta)$. As the simplest implementation, we take a set of bins labelled by p, then the total rate of signal or noise triggers in each bin is $r_{S,p}$ resp. $r_{N,p}$. The rate of signal triggers is estimated from O1-O2-O3 detections, up to a factor which relates the sensitivity of the active detector network to O3 sensitivity. The bins are initially taken over (template) chirp mass: an example set of boundaries is

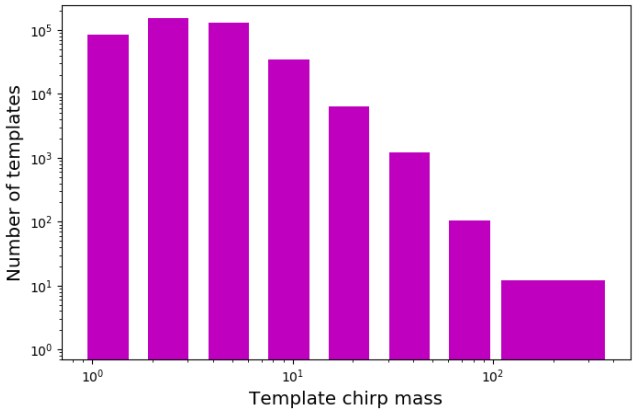

Figure 1: Binned template counts for a representative PyCBC Live bank.

$[0.87, 1.74, 3.48, 6.96, 13.92, 27.84, 55.68, 111.36, 500.0]\, M_\odot$, spaced by powers of 2 except for the highest bin.

For the background, assuming constant α_c, the false alarm rate of the search at a candidate ρ_c value is the integral of total background rate density R_N above ρ_c. Defining a total rate $r_{N,\mathrm{tot}}$ integrated over the whole bank, the FAR at ρ_c is $r_{N,\mathrm{tot}} \exp(-\alpha_c(\rho_c - \rho_{\mathrm{th}}))$, thus the rate density over ρ_c, also integrated over the whole bank, is $\alpha_c \times \mathrm{FAR}$. The distribution over templates is then modelled by taking the noise trigger rate to be proportional to the template count in each bin n_p^t, thus the noise rate density in bin p is

$$R_{N,p}(\rho_c) = \alpha_c \cdot \mathrm{FAR}(\rho_c) \frac{n_p^t}{\sum_p n_p^t}. \tag{7}$$

We show in Fig. 1 a representative set of binned template counts for a PyCBC Live template bank.

The effect of detector network sensitivity on signal rate is estimated via the BNS inspiral horizon $d_{h,D}$ for detector D (approximately 2.26 times the usually quoted "inspiral range"). Since the SNR of a signal at a physical distance d_L is proportional to $d_{h,D}$ (times mass-dependent and angular factors which on average are similar over detectors), the network SNR scales as

$$\rho_c^2 \propto d_L^{-2} \sum_D d_{h,D}^2. \tag{8}$$

The rate of signals detected above a SNR threshold ρ_{th} scales as the cube of the distance required to obtain a given network SNR, i.e.

$$r_S \propto \left(\rho_{\mathrm{th}}^{-2} \sum_D d_{h,D}^2 \right)^{3/2}. \tag{9}$$

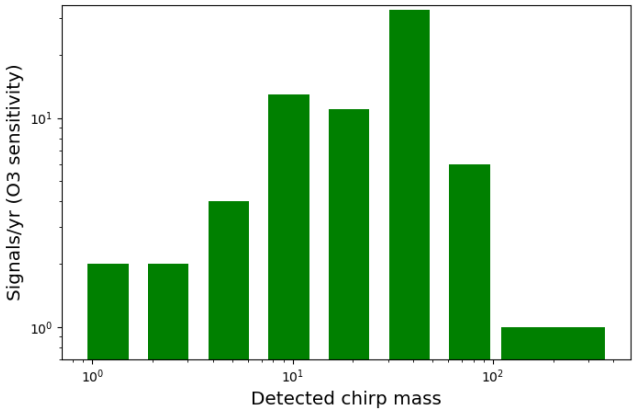

Figure 2: Binned signal counts for O1-O3 observations.

Thus, we approximate the total rate of signals above SNR threshold in bin p as

$$r_{S,p} = r_{p,\mathrm{O3}} \left(\sum_D d^2_{h,D} \right)^{3/2} \left(\sum_D d^2_{h,D(\mathrm{O3})} \right)^{-3/2}, \tag{10}$$

where the quantities labelled as 'O3' represent previous detection counts for signals above threshold, or O3 run representative horizon distances respectively. Figure 2 shows previous detection counts for observations up to O3; a typical reference network horizon distance, i.e. quadrature sum of $d_{h,D(\mathrm{O3})}$ over detectors, corresponding to BNS ranges of $[135, 110, 50]$ Mpc for LLO, LHO, Virgo respectively, is 410 Mpc.

We then have

$$\frac{p_{\mathrm{astro}}}{p_{\mathrm{terr}}} \simeq 3 \frac{\rho^3_{\mathrm{th}}}{\rho^4_c} \frac{r_{S,p} \sum_p n^t_p}{\alpha_c \cdot \mathrm{FAR}(\rho_c) n^t_p}. \tag{11}$$

The resulting p_{astro} value represents any and all astrophysical compact binary source classes, i.e. neutron star, black hole or mixed binaries; it is also of interest for followup observations to estimate the relative probabilities of different classes. In PyCBC Live, this is achieved by considering the search template chirp mass and an initial estimate of source redshift based on trigger SNR [8]. The resulting astrophysical class relative probabilities are multiplied by p_{astro} to obtain the absolute class probabilities included in public alerts, along with $p_{\mathrm{terr}} \equiv 1 - p_{\mathrm{astro}}$ [9].

4 Implementation of rate estimates

4.1 Event types and trials factors

The discussion so far has not accounted for effects due to the presence of several distinct event types generated by the Live search. Specifically, FAR is calculated/estimated for the event type of a given trigger, and is then multiplied by a trials factor to account for the number of types being produced; also, different event types are expected to see different signal rates (at a fixed SNR threshold) depending on relative detector sensitivities.

PyCBC Live produces both two-detector coincident and single-detector events: the background and FAR for coincident events is estimated via time-shifted analysis of the last few hours of data, while FAR for single-detector triggers is interpolated/extrapolated from an exponential fit to previous single trigger sets [3] (see also [10]). Given this significant method difference, trials are accounted for independently and separately for coincident vs. single triggers.

In single-detector time, only single events are produced and there is no trials factor. In double (two-detector) time only one coincidence type is produced, thus there is no trials factor for coincident events, but there is a trials factor of 2 for singles. In triple (three-detector) time three types of two-detector coincidence and three types of single exist. In addition, for coincident events the third detector is used in a "FAR followup" analysis which identifies the highest SNR peak within a physical time window around the triggers and assesses its significance relative to an off-source SNR time series [3]. This p-value for the 3rd detector SNR peak is then combined with the 2-detector FAR obtained via time slides to obtain a "combined" FAR. Finally, the smaller of the initial 2-detector FAR and the 3-detector combined FAR is chosen, with a further trials factor of 2. Hence, coincidence events in triple time have a total trials factor 6 as each 2-detector coinc may have its own "followup".

We would like to "reverse out" the FAR trials factor to obtain the noise trigger rate restricted to the event type of the candidate. Thus, in place of $\mathrm{FAR}(\rho_c)$ which includes a trials factor, we use $\mathrm{FAR}(\rho_c)/N_{tr,i}$ where $N_{tr,i}$ is the factor for event type i in the current observing time.

We also require some approximation of the relative signal rates between different event types. A hard-coded formula is used to estimate the relative signal rates, which can be checked against actual MDC injection recovery. The current formula for assigning relative signal rates is as follows:

1. In single-detector time, no correction is applied: the previous signal rate calculation is taken over.

2. For single triggers in multi-detector time, the 'horizon volume' for the triggered detector is compared to the sum of volumes over all detectors, plus a suppression factor $\sqrt{2}$ intended to represent fewer total signals found as singles than coincs. The total signal rate is multiplied by a factor

$$g_{\mathrm{single,D}} = \frac{(d_{h,D}/\sqrt{2})^3}{\sum_D d_{h,D}^3}. \tag{12}$$

3. For double coincs in multi-detector time, the "horizon volume" is determined by the less sensitive triggered ifo and we apply a factor

$$g_{\text{double}} = \frac{d^3_{h,<}}{d^3_{h,2}}, \tag{13}$$

where $d_{h,<}$ is the smaller horizon distance of the triggered ifos and $d_{h,2}$ is the second largest horizon distance out of all observing ifos, i.e. the largest possible $d_{h,<}$. This factor is always 1 in double time but may be < 1 in triple time for 'less sensitive' pairs of detectors.

4.2 FAR saturation

Consulting Eq. (11), we see that p_{astro} decreases with increasing signal SNR if the FAR is constant. This will occur for multi-detector events in the limit of signals which are ranked higher than all background samples, and thus are assigned a *limiting FAR* of 1 per background time, which for triple time is modified by the FAR followup and trials factors as above. As a result, loud signals may be assigned relatively low p_{astro}, not reflecting their likely origin. We aim to avoid this by "freezing" the ρ_c^{-4} and $\text{FAR}(\rho_c)^{-1}$ factors for coincident events which are at or beyond FAR_{lim} and have SNR above a chosen value $\rho_{c,\text{lim}}$ typical of signals that saturate the FAR estimate. Thus, for an event with $\rho_c > \rho_{c,\text{lim}}$ and $\text{FAR} \leq \text{FAR}_{\text{lim}}$, we replace the corresponding factors in (11) by $\rho_{c,\text{lim}}^{-4}$ and $\text{FAR}_{\text{lim}}^{-1}$. A similar procedure was followed for the O3 approximate online p_{astro} [11].

References

[1] B. P. Abbott *et al.* [LIGO Scientific and Virgo], "The Rate of Binary Black Hole Mergers Inferred from Advanced LIGO Observations Surrounding GW150914," Astrophys. J. Lett. **833** (2016), L1 doi:10.3847/2041-8205/833/1/L1 [arXiv:1602.03842]; B. P. Abbott *et al.* [LIGO Scientific and Virgo], "Supplement: The Rate of Binary Black Hole Mergers Inferred from Advanced LIGO Observations Surrounding GW150914," Astrophys. J. Suppl. **227** (2016), 14, doi:10.3847/0067-0049/227/2/14 [arXiv:1606.03939].

[2] A. H. Nitz, T. Dal Canton, D. Davis and S. Reyes, "Rapid detection of gravitational waves from compact binary mergers with PyCBC Live," Phys. Rev. D **98** (2018), 024050, doi:10.1103/PhysRevD.98.024050 [arXiv:1805.11174].

[3] T. Dal Canton, A. H. Nitz, B. Gadre, G. S. Cabourn Davies, V. Villa-Ortega, T. Dent, I. Harry and L. Xiao, "Real-time Search for Compact Binary Mergers in Advanced LIGO and Virgo's Third Observing Run Using PyCBC Live," Astrophys. J. **923** (2021), 254, doi:10.3847/1538-4357/ac2f9a [arXiv:2008.07494].

[4] A. H. Nitz, T. Dent, T. Dal Canton, S. Fairhurst and D. A. Brown, "Detecting binary compact-object mergers with gravitational waves: Understanding and Improving the sensitivity of the PyCBC search," Astrophys. J. **849** (2017), 118, doi:10.3847/1538-4357/aa8f50 [arXiv:1705.01513].

[5] G. S. Davies, T. Dent, M. Tápai, I. Harry, C. McIsaac and A. H. Nitz, "Extending the PyCBC search for gravitational waves from compact binary mergers to a global network," Phys. Rev. D **102** (2020), 022004, doi:10.1103/PhysRevD.102.022004 [arXiv:2002.08291].

[6] R. Lynch, M. Coughlin, S. Vitale, C. W. Stubbs and E. Katsavounidis, Astrophys. J. Lett. **861** (2018), L24, doi:10.3847/2041-8213/aacf9f [arXiv:1803.02880].

[7] R. Abbott *et al.* [LIGO Scientific and VIRGO], "GWTC-2.1: Deep Extended Catalog of Compact Binary Coalescences Observed by LIGO and Virgo During the First Half of the Third Observing Run," [arXiv:2108.01045].

[8] V. Villa-Ortega, T. Dent and A. C. Barroso, "Rapid source classification and distance estimation for compact binary mergers with PyCBC Live," Mon. Not. Roy. Astron. Soc. **515** (2022), 5718, doi:10.1093/mnras/stac2120 [arXiv:2203.10080].

[9] IGWN Public Alerts User Guide, `https://emfollow.docs.ligo.org/userguide/content.html#inference` (accessed May 2023).

[10] G. S. C. Davies and I. W. Harry, "Establishing significance of gravitational-wave signals from a single observatory in the PyCBC offline search," Class. Quant. Grav. **39** (2022), 215012, doi:10.1088/1361-6382/ac8862 [arXiv:2203.08545].

[11] LVK Software, `https://git.ligo.org/lscsoft/p-astro/-/blob/7d0e9d5c197fbdf183c4b3668d9a8c1b505be2a6/ligo/p_astro/computation.py#L203` (accessed May 2023).